Tor vergata Synoptic Solar Telescope: preliminary optical design and spectral characterization

Journal of Physics: Conference Series **1548** (2020) 012005 doi:10.1088/1742-6596/1548/1/012005

Tor vergata Synoptic Solar Telescope: preliminary optical design and spectral characterization

D Calchetti[1], G Viavattene[1], F Berrilli[1], D Del Moro[1], L Giovannelli[1] and M Oliviero[2]

[1] Università degli Studi di Roma "Tor Vergata", Via della Ricerca Scientifica 1, 00133 Rome, Italy
[2] INAF Osservatorio Astronomico di Capodimonte, Via Moiariello 16, 80131 Naples, Italy

E-mail: daniele.calchetti@roma2.infn.it

Abstract. Synoptic telescopes are fundamental tools in solar physics. They are tipically used for high cadence full-disk observations of the Sun at different wavelengths, in order to study the solar activity across the solar cycle. The TSST (*Tor vergata Synoptic Solar Telescope*) is a new synoptic telescope composed of a Hα filter-based telescope centered at 656 nm and a custom Magneto Optical Filter (MOF)-based telescope centered in the potassium (KI D1) absorption line at 770 nm. Observations of the Hα line are important for the detection of flaring regions and to track the Sun during the acquisition. The aim of the telescope is to monitor the solar activity using the line of sight (LoS) magnetograms and dopplergrams of the solar photosphere produced by the MOF-based telescope. Magnetograms are essential for the study of the geometry of the magnetic field in active regions, while dopplergrams can be used to study the dynamics of the solar lower atmosphere. In this work, we focus our attention on the custom MOF-based telescope. Firstly, we present the optical design of the instrument. It is a refractor telescope with a 80 mm aperture and an effective focal length of ∼1m. We also present details on the preliminary spectral characterization of this instrument at different cell temperatures, which is a mandatory step to calibrate magnetograms and dopplergrams. The results obtained during this first test are in agreement with the peaks separation (∼200 mÅ) and FWHM (∼ 50 mÅ) that we expected.

1. Introduction

The Tor vergata Synoptic Solar Telescope (TSST) project started in 2011 in collaboration with the research groups involved in the MOTH (*Magneto Optical filters at Two Height*) [1] experiment (at IfA-University of Hawaii, Georgia State University and JPL) and in the VAMOS (*Velocity And Magnetic Observations of the Sun*) [2] experiment (at INAF Observatory of Capodimonte). The core feature of this instrument is the simultaneous acquisition of dopplergrams and magnetograms of the solar photosphere provided by the Magneto Optical Filter (MOF)-based channel. A MOF [3, 4] is an excellent instrument to study the projection of the solar magnetic and velocity fields on the LoS. The MOF is an alkali-metal vapor cell with a strong (>1.2 kG) longitudinal magnetic field inside. The most common cells used in solar physics applications are based on sodium and potassium vapor [5, 6, 7], even if new MOF prototypes, based on calcium [8] and helium [9] vapor, have also been tested. The potassium and sodium MOFs allow us to observe two layers of the solar atmosphere: one between 300 and 400 km and the other between 600 and 700 km above the base of the photosphere. Moreover, the

MOF technology acquires images at high cadence, from 15 (as in the case of TSST) to 5 seconds [1]. This feature of the TSST telescope, which is necessary to follow the temporal evolution of solar active regions, represents an improvement compared to the existing instruments (HMI [10], GONG [11], VSM/SOLIS [12]), which actually produce dopplergrams and magnetograms either at only one layer in the solar atmosphere at a cadence greater than 30 s, or at two layers but at 2 min cadence.

To measure the magnetic and the velocity fields of the Sun along the LoS, one has to consider their effect on the solar spectrum. Specifically, the absorption lines get shifted by the Doppler effect and splitted by the Zeeman effect. The inverse Zeeman effect, induced by the LoS magnetic field of the Sun, splits the absorption line into several polarization states. If we consider a normal Zeeman effect, we will observe only two separate circular polarization states (σ^+ at lower wavelengths and σ^- at higher wavelengths) and one unshifted linearly polarized state (π) parallel to the magnetic field. The Doppler effect, induced by the LoS velocity field of the Sun, shifts the absorption line towards higher or lower wavelengths depending on the direction of the filed.

A MOF-based telescope can acquire consecutively four different images of the Sun in the red (R^+ and R^-) and blue (B^+ and B^-) wings of a given absorption line in both circular polarization states. If we consider a symmetric absorption line and the instrumental passband, we expect to observe the same intensity from the blue and red wing of the unperturbed line. If a magnetic or a velocity field is present in the region of line formation, we will measure a difference in the red and blue wing signal due to the split or to the shift of the line [13, 14]. Considering the Zeeman and the Doppler effect equations for wavelength shift, the four images can be combined together to obtain the uncalibrated dopplergram (D) and magnetogram (M) along the LoS [15]:

$$D = \frac{R^+ - B^+}{R^+ + B^+} + \frac{R^- - B^-}{R^- + B^-} \tag{1}$$

$$M = \frac{R^+ - B^+}{R^+ + B^+} - \frac{R^- - B^-}{R^- + B^-}\,. \tag{2}$$

These equations are proportional to the real LoS velocity and magnetic field. The calibration can be computed using the procedure in [2, 5, 16]. In particular, solar magnetograms are fundamental in space weather applications to study the evolution of the active regions. Synoptic telescopes, particularly when combined in a network, are mandatory to study the size, evolution and complexity of the active regions through the solar cycle [17, 18]. Magnetic proxies, such as magnetic fluxes and polarity separation lines derived from solar magnetograms, are used to assess the probability of space weather events from each active region [19]. Coronal mass ejection (CME) and flare forecasting need continuous multi-height measurements of the magnetic field of the Sun, so synoptic observations are essential for space weather [20, 21, 22, 23]. On the other side, dopplergrams are very important to study subsurface flows, the interior of the Sun and the propagation of waves in the solar atmosphere [24, 25].

In Sect. 2 we present a general overview of the TSST, together with the preliminary optical design and spectral characterization of the MOF-based channel. The conclusions are provided in Section 3.

2. Tor vergata Synoptic Solar Telescope (TSST)

The new TSST will be a double-channel synoptic telescope and it will represent one of the nodes of a network of solar observatories, together with the MOTH and the VAMOS telescopes, to provide multi-height observations for space weather applications at a cadence of 15 seconds. The telescope is now in the assembling phase and the first light is planned in the spring of 2020. It is composed by an Hα channel and a custom potassium (KI D1 line) MOF channel. The Hα

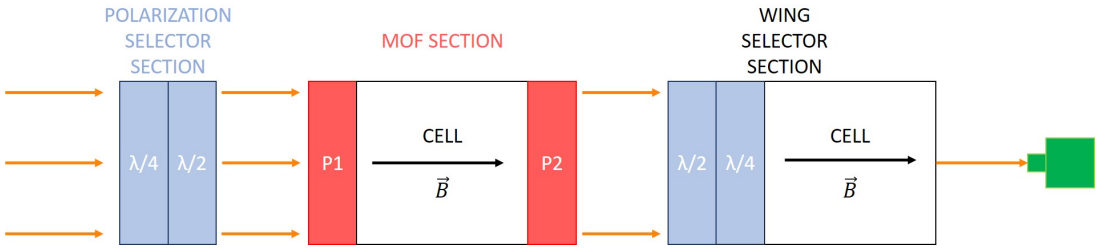

Figure 1. Scheme of the TSST MOF channel. A quarter-waveplate and a rotating half-waveplate select the polarization state. A potassium MOF between two crossed polarizers provides a passband with peaks in the blue and red wings of the KI D1 absorption line. A rotating half-waveplate, a quarter waveplate and a potassium MOF select the blue or the red wing passband alternatively absorbing the other.

channel will be a refractor telescope with a clear aperture of 127 mm and a temperature-stabilized etalon with 0.4 Å passband in collimated configuration. The flaring regions are clearly visible in the Hα band, particularly during the impulsive and flash phases of the flare events, when the intensity and the bandwidth increase reaching the maximum at the end of the flash phase [26]. Therefore, the images acquired with the Hα channel will be used for real-time detection of flare regions. This instrument will also be a part of the solar tracking system by image processing during the observation (similar to [27]).
The MOF-based telescope will be a custom refractor telescope. The spectro-polarimetric selection scheme will be similar to that of the VAMOS telescope, and it is shown in Fig. 1. Its main constituencies are described in the following.

- The Polarization Selector (PS) section rotates the incoming circularly polarized light in the KI D1 line (induced by the solar magnetic field) with a rotating half-waveplate and a fixed quarter-waveplate, so that only one polarization state can pass through the following section as linearly polarized light.
- The MOF section, where the metal vapor and the strong longitudinal magnetic field inside the cell induce inverse Zeeman effect and Macaluso Corbino effect (a Faraday rotation in proximity of resonance lines) in the wings of the KI D1 absorption line. The inverse Zeeman effect absorbs 50% of the incoming light at the $\sigma^{\pm}$ wavelengths, while the Macaluso Corbino effect rotates the linear polarization between and outside the Zeeman absorption. The two linear polarizers P1 and P2 are crossed, therefore they cut off all the spectrum, except for those wavelengths for which the MOF rotates or changes the polarization. The MOF section defines the typical shape of the MOF passband (see Fig. 3, discussed later) with two peaks in the red and blue wing of the absorption line.
- The Wing Selector (WS) section, in which only the inverse Zeeman effect occurs. Its purpose is that of letting the blue or red wing to pass alternatively [28].

2.1. Preliminary Optical Design

The optical scheme of the MOF telescope, shown in the left panel of Fig. 2, is basically a double Keplerian telescope with an imaging lens. The objective lens is a *Spindler & Hoyer* with a diameter of 80 mm and a focal length of 1185 mm. Three pre-filters are inserted in the converging solar beam produced by the objective lens: an IR cut filter (>825 nm), a UV cut filter (<700 nm), and a wide potassium filter (41 nm bandwidth centered at 769 nm) used to reject most of the solar radiation. Four identical achromatic doublets (50 mm of diameter and 200 mm of focal length) are then used to collimate, re-image, collimate again and focus the Sun

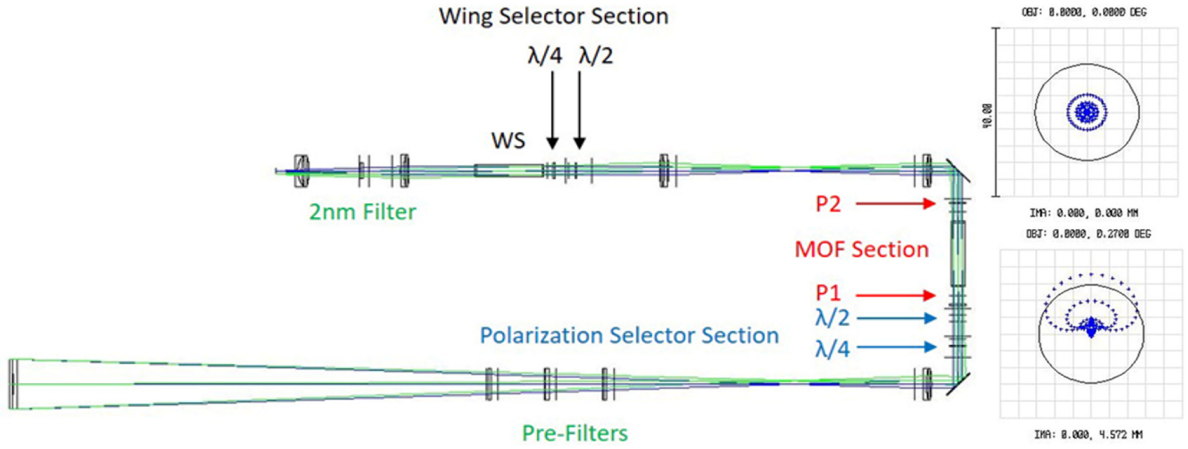

Figure 2. *Left Panel*: optical design of the double Keplerian MOF-based telescope. *Right Panel*: spot diagram of the MOF-based telescope. The top diagram refers to the rays from the center of the Sun, while the bottom diagram is produced by the rays from the limb. The Airy disk, shown as a solid black circle, has a diameter of ∼2 arcsec.

image on the CMOS (Complementary Metal-Oxide Semiconductor) camera. The PS Section and the MOF Section are placed in the first collimated part. The WS section (half-waveplate, quarter-waveplate and WS cell) is placed in the second collimated part of the optical beam. A 2 nm bandwidth interference filter is placed after the imaging lens in order to define the working wavelength range. A bi-convex lens and a plane-concave lens are placed before the camera to compensate distortions and to flatten the image. Two flat mirrors are used to fold the light path and to reduce the size of the instrument.
The spot diagrams for the center and for the edge of the field of view are reported in Fig. 2 (right panel): at the center the image is diffraction limited. Since the pixel scale will be ∼3 arcsec/px using a 1k×1k pixels camera, we are sub-sampling the image since the diffraction limit is at 2 arcsec, thus the minor distortions at the image edge will not affect the image quality.
All the optical path will be closed in a thermostatic enclosure in order to avoid the dilatation of the optical bench and the two MOF and WS cell will be closed in further thermostatic enclosures to keep the temperatures of the two cells stable. The latter is very important in order to avoid optical aberration generated by the change in the distances between the optical elements and to prevent changes in the passband of the telescope that is very sensitive to the temperature (as shown in Fig. 3 and 4).

2.2. Preliminary Spectral Characterization

We perform a first spectral calibration of the MOF and WS cells to find the best passband of the instrument. Since the Zeeman effect depends on the magnetic field while the Macaluso Corbino effect is strongly dependent on the density of the vapor (therefore on the temperature), we set the magnetic field and the temperature of the cells in such a way to:

- match the bandpass of the WS with the MOF peaks;
- obtain a distance of ∼200 mÅ between the peaks in the blue and red wing.

During the preliminary tests, we only measured the red wing passband via a tunable laser system. These tests aimed to verify the proper functioning of the cells and to measure the spectral properties of the MOF section and of the WS. The optical setup consisted in the MOF section, a quarter-waveplate and the WS. Once set the correct MOF temperature, we measured

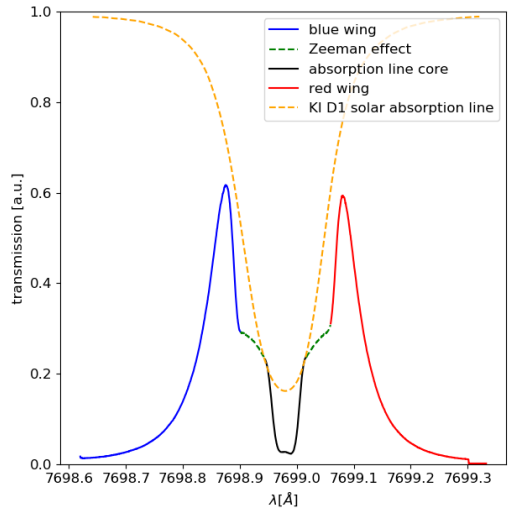

Figure 3. Measured MOF passbands. Blue and red lines are the Macaluso Corbino Peaks, green dashed line is due to the inverse Zeeman absorption, yellow dashed line is the reference solar absorption line.

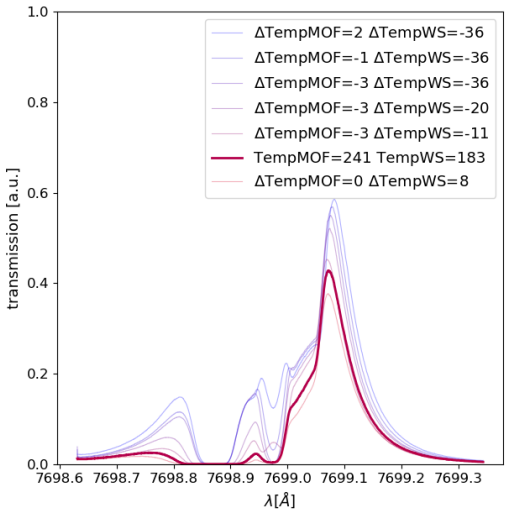

Figure 4. Red wing passbands for different WS temperatures separated by ∼10°C and at MOF temperatures close to operating one. The MOF and WS magnetic flux densities are 1.23 kG and 2.26 kG, respectively.

the MOF passband with the WS turned off (no absorption after MOF section) shown in Fig. 3. We can recognize the red and blue peaks, the MOF inverse Zeeman absorption and the central absorption due to the π polarization state of the core of the spectral line, which has a polarization vector parallel to the magnetic field (i.e. to the LoS). Therefore, the π state is not observable using a longitudinal magnetic field in the cell. We analyzed the effect of the WS temperatures on the instrument passband. Fig. 4 shows how different WS temperatures affect the red wing passband. The measured FWHM is 65 mÅ, the transmission peak reaches 43% and the separation between the peaks is 205 mÅ. Furthermore, the sidelobes have a measured passband of 2.5%. This quantity is important to compute the amount of spurious signal and the cross-talk in the final dataset and to increase the signal to noise ratio of our maps. Using this passband and considering the whole 2 nm band of the telescope, we can simulate a magnetic and velocity signal from the Sun by splitting and shifting the potassium line. This simulation allows us to compute the velocity and magnetic maps considering the real passband, so we can evaluate the cross-talk between the magnetic field and the dopplergram, and we can also measure the linearity between the measured Doppler signal and the simulated velocity. This step is fundamental for the calibration of the dopplergrams [5] and magnetograms [16] and will be completed after the telescope assembly, in order to obtain the complete passband and to measure spurious signals generated by all the optical elements.

3. Conclusion

We presented the Tor vergata Synoptic Solar Telescope (TSST) that is able to acquire velocity and magnetic field maps of the solar atmosphere. These maps are necessary for space weather applications (flare and CME forecasting), especially if associated with an Hα channel to detect flaring events in real time. Specifically, we showed the preliminary optical design and spectral characterization of the potassium MOF-based channel of the TSST. The custom optical design

allows us to reach a good spatial resolution and a very narrow passband (see [2, 28]). The spectral characterization of the cells demonstrates that we can reach an high transmission peak (43%) and a very narrow passband (FWHM = 43 mÅ). In the future, we will upgrade the temperature controller of the cells to improve the thermal stability. We will repeat the test after the telescope assembly to thoroughly characterize the instrument: we will measure the definitive passband, verify the sensitivity of the computed magnetograms and dopplergrams, and detect possible spurious polarization signals from the optical elements of the telescope.

References

[1] Forte R, Jefferies S M, Berrilli F, Del Moro D, Fleck B, Giovannelli L, Murphy N, Pietropaolo E and Rodgers W 2018 *Space Weather of the Heliosphere: Processes and Forecasts* (*IAU Symposium* vol 335) ed Foullon C and Malandraki O E pp 335–339
[2] Oliviero M, Severino G and Esposito G 2010 *Ap&SS* **328** 325–329
[3] Cimino M, Cacciani A and Sopranzi N 1968 *Sol. Phys.* **3** 618–622
[4] Agnelli G, Cacciani A and Fofi M 1975 *Sol. Phys.* **44** 509–518
[5] Oliviero M, Severino G and Straus T 1998 *Mem. Soc. Astron. Italiana* **69** 623
[6] Berrilli F, Velli M, Roselli L, Bigazzi A and ADAHELI Team 2009 *Mem. Soc. Astron. Italiana* **80** 251
[7] Haberreiter M, Finsterle W and Jefferies S M 2007 *Astronomische Nachrichten* **328** 211
[8] Rodgers W, Murphy N and Jefferies S M 2005 *AGU Spring Meeting Abstracts* vol 2005 pp SH13C–13
[9] Murphy N, Smith E, Rodgers W and Jefferies S 2005 *Solar Wind 11/SOHO 16, Connecting Sun and Heliosphere* (*ESA Special Publication* vol 592) ed Fleck B, Zurbuchen T H and Lacoste H p 511
[10] Scherrer P H *et al.* 2012 *Sol. Phys.* **275** 207–227
[11] Harvey J W *et al.* 1996 *Science* **272** 1284–1286
[12] Henney C J, Keller C U and Harvey J W 2006 *Solar Polarization 4* (*Astronomical Society of the Pacific Conference Series* vol 358) ed Casini R and Lites B W p 92
[13] Landi Degl'Innocenti E 2004 *Fisica Solare* (Milan: Springer)
[14] Stenflo J O 1978 *Reports on Progress in Physics* **41** 865–907
[15] Cacciani A, Ricci D, Rosati P, Rhodes E J, Smith E, Tomczyk S and Ulrich R K 1990 *Nuovo Cimento C Geophysics Space Physics C* **13** 125–130
[16] Vogt E, Oliviero M, Severino G and Straus T 1999 *Magnetic Fields and Solar Processes* (*ESA Special Publication* vol 9) ed Wilson A and et al p 405
[17] Elsworth Y, Broomhall A M, Gosain S, Roth M, Jefferies S M and Hill F 2015 *Space Sci. Rev.* **196** 137–166
[18] Toriumi S and Wang H 2019 *Living Reviews in Solar Physics* **16** 3
[19] Schrijver C J 2007 *ApJ* **655** L117–L120
[20] Piersanti M *et al.* 2017 *Solar Physics* **292** 169
[21] Falconer D, Barghouty A F, Khazanov I and Moore R 2011 *Space Weather* **9** S04003
[22] Kilpua E K J, Lugaz N, Mays M L and Temmer M 2019 *Space Weather* **17** 498–526
[23] Berrilli F *et al.* 2017 *Proceedings of the International Astronomical Union* **13** 348351
[24] Basu S 2016 *Living Reviews in Solar Physics* **13** 2
[25] Khomenko E and Collados M 2015 *Living Reviews in Solar Physics* **12** 6
[26] Benz A O 2017 *Living Reviews in Solar Physics* **14** 2
[27] Lee C D, Huang H C and Yeh H Y 2013 *Sensors* **13** 5448–5459
[28] Tomczyk S, Streander K, Card G, Elmore D, Hull H and Cacciani A 1995 *Sol. Phys.* **159** 1–21